

A 60 GHz Dual-Polarized Probe for Spherical Near-Field Measurements

Muntianu, Paula Irina; Breinbjerg, Olav

Published in:

Proceedings of 39th Annual Symposium of the Antenna Measurement Techniques Association

Publication date:
2017

Document Version
Peer reviewed version

[Link back to DTU Orbit](#)

Citation (APA):

Popa, P. I., & Breinbjerg, O. (2017). A 60 GHz Dual-Polarized Probe for Spherical Near-Field Measurements. In Proceedings of 39th Annual Symposium of the Antenna Measurement Techniques Association

DTU Library

Technical Information Center of Denmark

General rights

Copyright and moral rights for the publications made accessible in the public portal are retained by the authors and/or other copyright owners and it is a condition of accessing publications that users recognise and abide by the legal requirements associated with these rights.

- Users may download and print one copy of any publication from the public portal for the purpose of private study or research.
- You may not further distribute the material or use it for any profit-making activity or commercial gain
- You may freely distribute the URL identifying the publication in the public portal

If you believe that this document breaches copyright please contact us providing details, and we will remove access to the work immediately and investigate your claim.

A 60 GHz Dual-Polarized Probe for Spherical Near-Field Measurements

Paula Irina Popa, Olav Breinbjerg
Department of Electrical Engineering
Technical University of Denmark

Oersteds Plads, building 348, DK-2800 Kgs. Lyngby, Denmark

Abstract—Dual-polarized probe systems can be used with some of the advantages: the two electric field components are simultaneously measured within a single scan, amplitude and phase drift affects the two polarization components in the same way, and there is no need for mechanical rotation of the probe. In this work we design and test a dual-polarized probe system at 60 GHz - a conical horn, including the elements: SPDT (single pole double throw) switch, an OMT (orthomode transducer) both components with 40 dB isolation - a square to circular transition (3.75 mm to 3.58 mm), cables and two coaxial to waveguide adapters up to 67 GHz for OMT-switch connection. A 27 dBi gain conical horn is designed by using WIPL-D software and in-house manufactured. The 60 GHz probe system is being assembled and tested in planar near-field (PNF) setup at DTU. The results are validated by comparison with WIPL-D simulations, showing a good agreement within the validity region, down to -30 dB pattern levels. Channel balance is carried out to compensate for the amplitude and phase differences between the signals at the OMT ports.

I. INTRODUCTION

Literature studies show that millimeter-wave (mm-wave) dual-polarized probes for spherical near-field antenna measurements have been developed up to 40 GHz [1], and different spherical near-field (SNF) antenna measurement setups at mm-waves above 100 GHz have been implemented ([2],[3]), which involves probe rotation either by swing or robotic arm, being responsible for switching between the probe polarizations. However, there are no dual-polarized probes for SNF antenna testing, which simply rely on OMTs (orthomode transducers) developed at 60 GHz. To ensure accurate near-field antenna measurements at mm-waves, a dual-polarized probe with the following characteristics is required: good polarization purity (cross-polar level lower than that of the antenna under test - AUT), high port to port isolation, "proper" pattern shape, low reflection coefficient, wide bandwidth and high gain. At mm-waves cross coupling for OMTs and switches typically increases, and this is not acceptable in order to accurately measure the AUT cross-polarization component. However, lately progress of the electronic products in the mm-wave band opens the way for using the necessary hardware components with the right characteristics for 60 GHz dual-polarized probe implementation. Path loss is higher at mm-waves reducing the system dynamic range for the measured data and in order to compensate for it, a high gain probe is desired.

In this paper we present a first-order dual-polarized probe implemented at 60 GHz for spherical near-field measurements.

First-order $\mu = \pm 1$ rotationally symmetric probe is desired because it employs an efficient data-processing and measurement scheme. A conical horn is designed by carrying out WIPL-D [7] simulations and then in-house manufactured. The probe system components were procured and their S-parameters individually tested. In section II the probe system individual components and testing results are presented.

Section III includes temperature drift and flexing cable effect of the PNF setup investigation, as these represent sources of uncertainties in mm-wave near-field antenna measurements.

The probe system is being assembled and tested as an AUT in the planar-near field setup (PNF) at DTU. In section IV first tests of the probe system are presented. These involve full-scan measurements in the (40-60) GHz band of the co- and cross-polar components over an 200×200 mm² area without the switch - including the conical horn, the transition and the OMT, and in the next stage, measurements with the switch. The probe test measurements results are validated by comparison with WIPL-D simulations.

In section V channel balance measurements results are shown, for two consecutive amplitude phase factors measurements conducted in the PNF setup.

II. PROBE COMPONENTS

The probe system components are: a 27 dBi conical horn, an OMT, a circular to square transition, a SPDT switch, two connecting cables and two coax to waveguide adapters. In the following these components will be described individually.

A. Conical horn

For spherical near-field measurements a probe pattern containing $\mu = \pm 1$ spherical modes is required in order to employ a practical data processing and measurement scheme. This requirement is satisfied by rotationally symmetric conical horns in which the TE₁₁ mode is excited. Another important aspect is that the path loss at 60 GHz for a 6 m distance (the distance between the probe and AUT in DTU-ESA Facility) is 83 dB and represents 15 dB additional loss compared to for example 10 GHz for which the path loss is 68 dB. Therefore a 27 dBi gain conical horn is employed as the probe to compensate for the path loss and to fulfill the probe $\mu = \pm 1$ pattern requirements. This value of the gain is obtained based on a study of the existing dual-polarized probes at DTU-ESA Facility in the (3-18) GHz band, involving calculation

of the gain as a function of the probes aperture and of the path loss as a function of the probes central wavelength. The conical horn is designed by conducting simulations in WIPL-D (Fig.1). TE₁₁ mode is assigned to the horn using waveguide mode excitation. To get a 27 dBi gain, the horn dimensions - obtained from simulations - are 52 mm aperture diameter and 187 mm the horn length. The horn circular waveguide size is 3.58 mm, the standard waveguide size for the WR-15 band. The horn is then in-house manufactured (Fig.2).

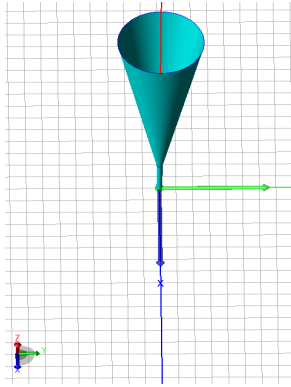


Fig. 1. Design of the 60 GHz conical horn in WIPL-D

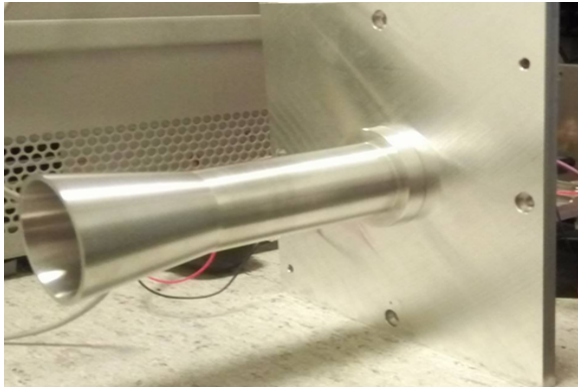


Fig. 2. 60 GHz manufactured conical horn

B. OMT and transition

In order to be able to connect the OMT square shape antenna port with 3.75×3.75 mm size to the conical horn port with the circular waveguide size of 3.58 mm of the conical horn, a square to circular transition is acquired from Sage-Millimeter (Fig. 3). A 50-75 GHz OMT with 40 dB isolation is procured from Sage-Millimeter and tested. The OMT has two ports ports p_1 and p_2 in addition to the square shape antenna port (Fig.3). The OMT S-parameters were measured with the conical horn attached to the antenna port, showing values lower than -40 dB for the port-to-port coupling in the whole band (except at 58 GHz) (Fig.4). S_{11} parameter is measured at - p_1 port, showing values below -15 dB. However, at the other port of the OMT - port p_2 , the measured return loss is above -6 dB at

60 GHz (Fig. 4). This very high value of S_{22} may be due to a manufacturing error, but the communication from the vendor never clarified this completely. These very different S-parameters for the two ports will of course be manifest in the channel balance; see section V.

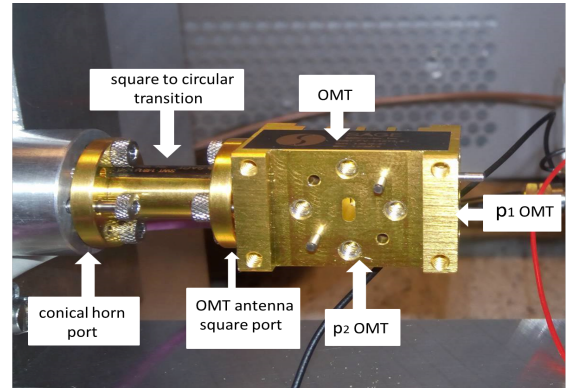


Fig. 3. Square to circular transition and OMT

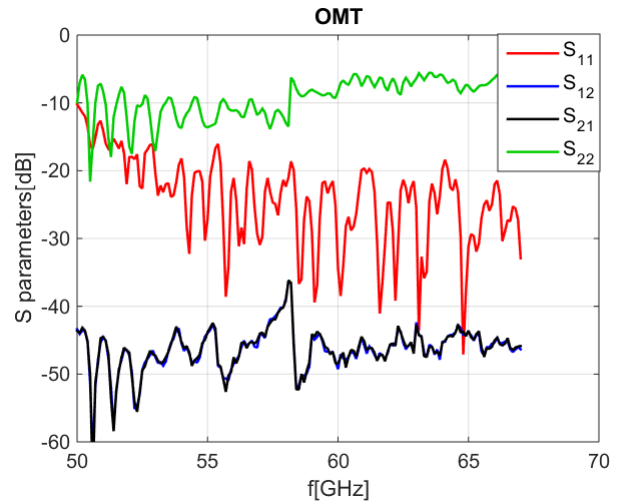


Fig. 4. Measured S parameters of the OMT

C. SPDT switch and connecting components

In order to simultaneously measure the vertical and horizontal polarization components of the field a switch with good isolation is required. A SPDT (Single Pole Double Throw) switch from Ducommun is procured working within 600 MHz-67 GHz band. The minimum isolation at 60 GHz is around -40 dB (measured) and the insertion loss measurement shows values around -9 dB above 50 GHz (Fig 5). The switch control is ensured by the TTL input which selects between J_2 , J_3 ports by changing between the voltage levels - 0 V - TTL low - J_1J_2 ports are activated - and 5 V - TTL high - J_1J_3 ports are selected. The switching speed is 150 ns and the RF port is at J_1 (Fig 6). The measured S-parameters of the switch are shown in Fig.5 for the insertion loss state, when

TTL is low (J_1J_2 is selected) and when TTL is high (J_1J_3 is selected). For simplicity the isolation is shown only when J_1J_2 port is activated, showing values below -40 dB in the whole band. To connect the switch with the OMT two coax to waveguide adapters working within 50-75 GHz band with 1.85 mm connectors, and two cables operating up to 67 GHz with 25 mm length each are acquired from Flann Microwave. Cables tests results indicate values below -20 dB and around -2.5 dB in the whole band for the reflection coefficients and insertion loss (Fig.7).

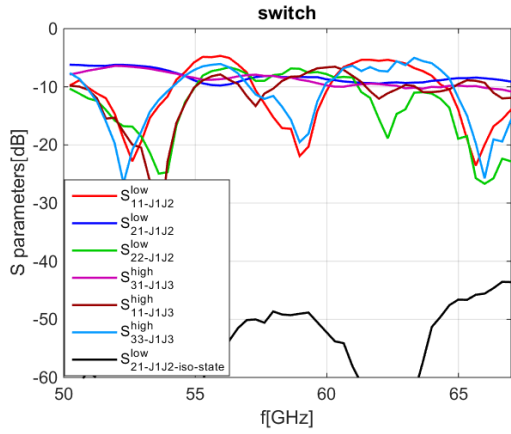


Fig. 5. Measured S parameters of the SPDT switch

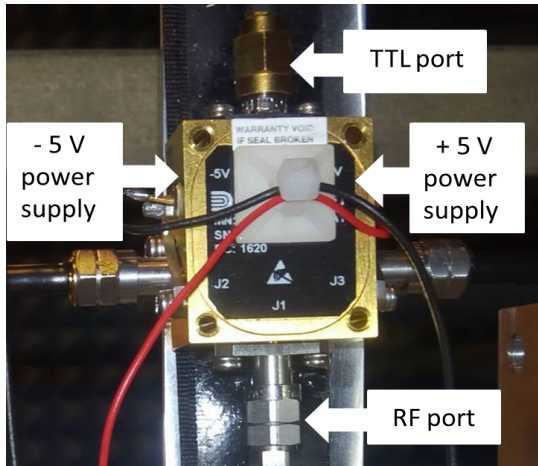


Fig. 6. SPDT switch

III. PROBE SYSTEM

The 60 GHz probe components described in the 'Probe components' section is assembled (Table 1, Fig. 8, Fig.9) and tested as an AUT in the PNF setup at DTU. The two cables are connecting port p_1 of the OMT with port J_2 of the switch and port p_2 of the OMT to port J_3 of the switch using the coaxial to waveguide adapters. For TTL low - J_1J_2 ports are activated and - for TTL high - J_1J_3 ports are selected. The switch is fed by two power supplies which provide +5 V and -5 V voltage

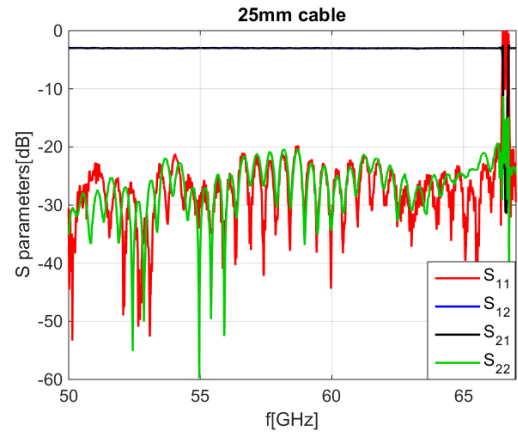


Fig. 7. Measured S-parameters of the cables connecting the switch and OMT

levels. The 3.75 mm to 3.58 mm square to circular transition is integrated between the conical horn and the OMT.

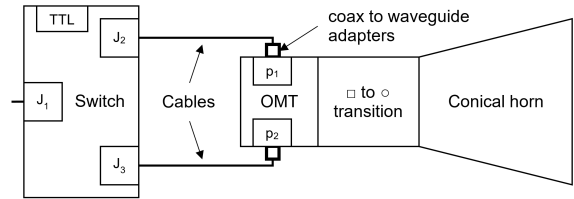


Fig. 8. Probe system schematic

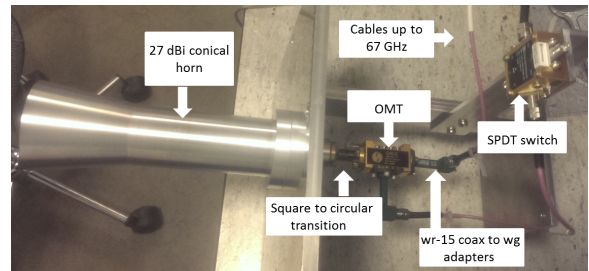


Fig. 9. Assembled probe system

TABLE I
PROBE COMPONENTS

Components	Company manufacturer
broadband SPDT PIN diode switch	Ducommun
OMT SAT-FV-14815	Sage Millimeter
cables GC08	Flann Microwave
adapters 25373-VF50	Flann Microwave
square to circular transition SWT-148141	Sage Millimeter
27dBi conical horn	In-house manufactured

A. Measurement setup

The probe system is tested as an AUT in the Planar Near-Field (PNF) setup without external frequency conversion

upgraded up to 60 GHz [6]. As the probe, an open ended circular waveguide (OECW) is used operating in the (40-60) GHz band. Two 1.5 m cables working up to 65 GHz from Pasternack are used to connect the OECW and the AUT to the E8361A Agilent Vector Network Analyzer (VNA). The OECW is connected to an OMT from Millitech [8], used in one polarization, operating within 40-60 GHz band. The probe is 90° manually rotated to switch between the polarizations.

B. Uncertainty Investigation

Before testing the probe system as an AUT, measurement tests are conducted in order to verify the potentially sources of uncertainty present in the setup. Since no external mixers are included in the system, flexing cable effect is investigated at 60 GHz by measuring the return loss along the cable connected to the moving OMT which is shortcircuited at the antenna port. The reflection coefficient measurement is conducted over a $200 \times 200 \text{ mm}^2$ scan area, with 2.4 mm sampling step and thus 83×83 sampling points. The measurement time with these settings is around 8 hours. The effect of flexing on cable properties is investigated by verifying the phase variation of the transmission loss S_{21} expressed as the difference between the measured S-parameter of the cable S_{11} -when the cable S parameters were tested - and the reflection coefficient measured when the cable was moving and connected to the OMT. The results indicate no variation along horizontal axis and around 5° along the vertical. The latter is most likely caused by the fact that the cable shape variation is more pronounced over the vertical scan area as compared to the horizontal one. However since this is a two way measurement, it can be concluded that the phase variation is only half, thus around 2.5° over the vertical direction. As the duration of a measurement for one polarization is around 8 hours the thermal drift effect is investigated at 60 GHz by measuring the signal every minute over 8 hours, with the AUT and OECW probe positioned in front of each other. The first hour is disregarded due to the VNA warm-up effects. The results show small amplitude and phase variation; 0.18 dB peak to peak variation, 0.02 dB standard deviation (1σ) and a mean value of around -43 dB for the amplitude, while the phase drift indicates 1.5° peak to peak variation, with a mean value of -38° and 0.77° (1σ) standard deviation (Fig.10). It can be noted that the thermal drift effect is minor in the PNF setup.

Results repeatability were investigated by carrying out two full consecutive scans at 60 GHz of an AUT which will be described in the following, over an area of $200 \times 200 \text{ mm}^2$, 2.4 mm sampling step in vertical and horizontal directions, with 8 hours the duration of a scan. The first measurement was started in the afternoon and finished during the night, while the second scan was started the next day in the morning. After the first measurement was carried out, the cables from the AUT and probe were disconnected from the VNA to initialize the scanner and then reconnected back before the second measurement was conducted, as they are not long enough to reach the reset position. To verify the differences between the

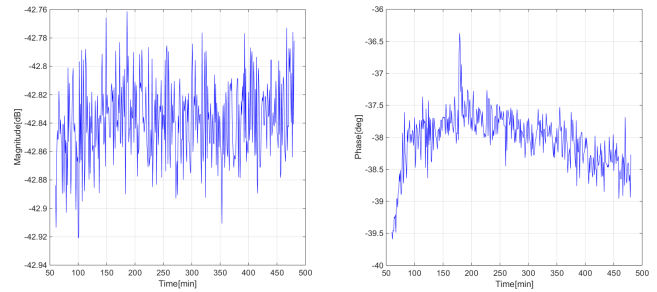


Fig. 10. Amplitude (left) and phase (right) drift over 7 hours (first hour excluded)

far-field patterns of the two measured signals (S1 and S2), the equivalent error signal (EES) is calculated with (1) for the E and H planes (Fig. 11).

$$EES = 20 \log_{10} |10^{S1_{dB}/20} - 10^{S2_{dB}/20}| \quad (1)$$

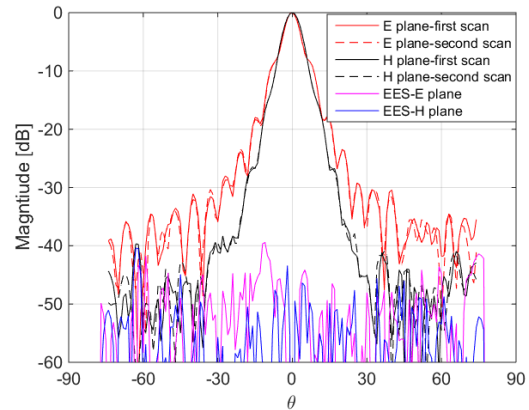


Fig. 11. Radiation pattern of two repeatability measurements and EES levels for E ($\phi = 0^\circ$) and H ($\phi = 90^\circ$) planes

The results show a low EES level below -40 dB, with a mean value of around -60 dB and a standard deviation of 15 dB, and thus a good repeatability of the measured data.

IV. PROBE SYSTEM TESTING

A. Measurements and simulations

The 60 GHz probe system is tested as an AUT in the PNF setup, without the switch at the first stage by measuring the co- and cross polar components at each port of the OMT (p_1 and p_2) resulting in four measured signals: Co-OMT p_1 , Co-OMT p_2 , Cross-OMT p_1 and Cross-OMT p_2 . (Fig.12, Fig.13) The OECW probe was manually 90° rotated to measure the cross polar components of the AUT. Probe correction was applied on the measured data and channel balance was assumed to be 1. Each measurement was conducted over a $200 \times 200 \text{ mm}^2$ scan area, with a 2.4 mm sampling step in horizontal and vertical directions, for 83×83 sampling points the duration of one scan being around 8 hours. For this scan

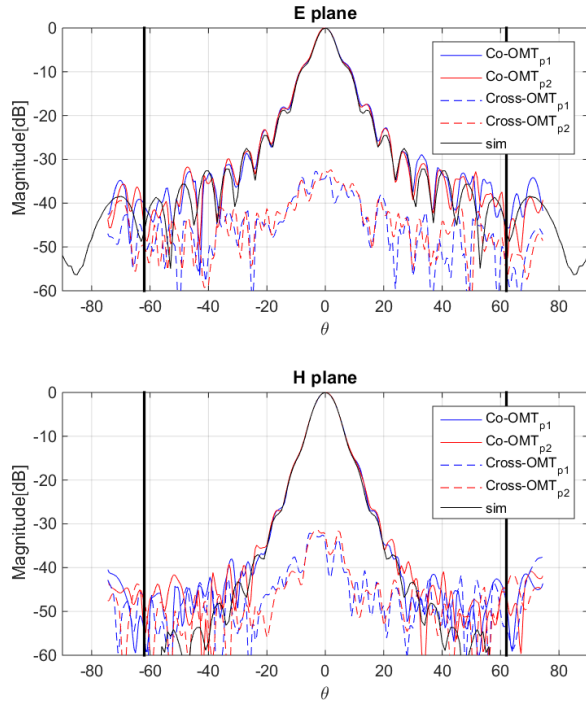


Fig. 12. 60 GHz probe system (AUT) radiation pattern: measurements (without the switch) and simulations for E (top) and H (bottom) planes

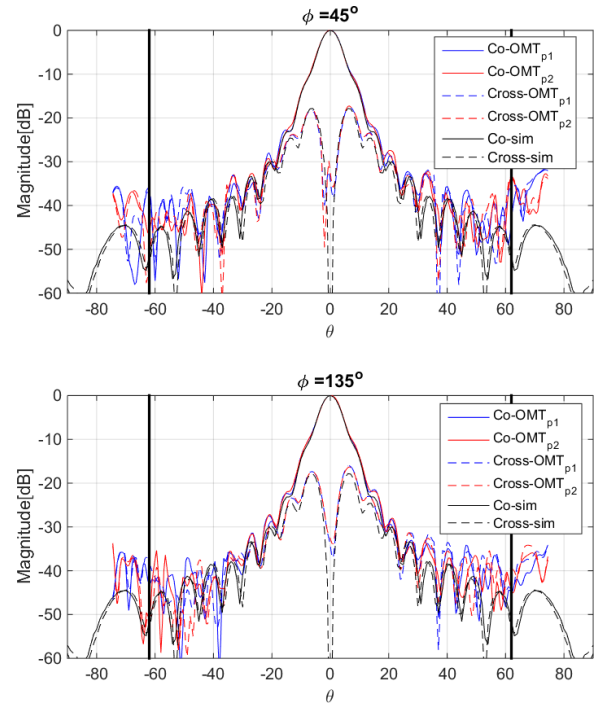


Fig. 13. 60 GHz probe system (AUT) radiation pattern: measurements and simulations for 45° (top) and 135° (bottom) planes

area size, with 52 mm conical horn diameter and a probe-AUT distance of 40 mm, the validity region is calculated to be about $\pm 62^\circ$ and it is marked within the two vertical black lines (Fig.12, Fig.13). The results are validated by comparison with WIPL-D simulations of the conical horn - in which the transition, OMT and switch are not included - in four planes: $\phi = 0^\circ$, $\phi = 90^\circ$, $\phi = 45^\circ$ and $\phi = 135^\circ$. (Fig.12, Fig. 13). It can be noted that there is a good agreement within the main beam region between the co-polar patterns measured at p_1 and p_2 of the OMT and the WIPL-D simulations of the conical horn for all four planes, with some differences at pattern levels lower than -30 dB, which are likely to be caused by various sources of uncertainty in the PNF setup, such as noise and reflections from the room as the absorber treatment in the PNF setup is quite poor. The cross-polar components for the E (0°) and H (90°) plane of the measured data show peak values of around -34 dB at p_1 of the OMT and -32 dB at p_2 of the OMT, and for θ angles larger than 10° , the cross-polar level is below -40 dB. Some possible explanations for the asymmetric cross-polar components of the E and H plane are sources of uncertainty present in the PNF setup such as mechanical misalignment.

The measured and simulated cross-polar components for 45° and 135° cuts (Fig.13) indicate a very good agreement within the angular region of validity, with a minimum level on axis. In general it can be noted that the measured and simulated data show a good agreement for 0° , 45° , 90° and 135° planes, with differences at lower pattern levels. Some possible explanations for these small differences are the uncertainty sources present

in the PNF setup, and the fact that the outer probe structure was not included in the simulations (absence of transition, OMT and switch from the WIPL-D design).

B. Measurements with switch

To test the switch effect integration in the probe system, the co- and cross polar components are measured when TTL switch port is low (J_1J_2 is activated) and when TTL is high (J_1J_3 is activated) resulting in four measured signals: Co-switch $^{low}_{TTL}$, Co-switch $^{high}_{TTL}$, Cross-switch $^{low}_{TTL}$ and Cross-switch $^{high}_{TTL}$ (Fig.14). The measurement results are compared to the data obtained from the measurements conducted without the switch - with OMT. The scan area, sampling step and probe AUT distance settings are kept identical to the ones introduced when the AUT radiation pattern was measured without the switch. The co-polar components show a good agreement within the main beam region down to -20 dB/-30 dB. It can be noted that at θ angles larger than 20° (Fig. 14) the side lobes levels are higher for the data measured with the switch than without the switch. A possible explanation for this is that the switch introduces extra losses (around -9 dB measured at 60 GHz), so the overall noise level is higher and the measured signal level is lower when the switch is connected to the probe system. The cross polar components of the data measured with the switch indicate levels below -30 dB and a peak value of -39 dB when TTL is low -port J_2 is connected to OMT p_1 and around -32dB when TTL is high and port J_3 is connected to OMT p_2 .

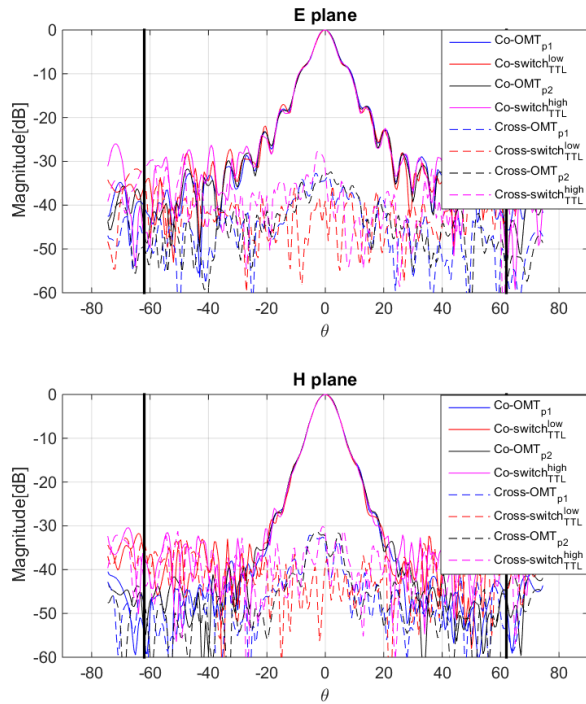


Fig. 14. 60 GHz radiation probe system (AUT) pattern measurements with the switch and without switch (OMT) for E (top) and H (bottom) planes

C. Channel balance

As the reflection coefficient of p_2 of the OMT is quite high (around -6 dB at 60 GHz), in order to compensate for the amplitude and phase differences between the two signals at port p_1 and port p_2 of the OMT, channel balance is carried out. The AUT and OECW probe are horizontally polarized and the signal S1 at port J_2 of the switch (connected to p_1 of the OMT) is measured. Then the probe is 90° rotated and the switch is flipped, allowing the signal S2 to be measured at port J_3 of the switch (connected to p_2 of the OMT). The ratio $S1/S2$ - the amplitude phase factor A_{xy} - is measured and then if needed this value will be applied on the data to correct for the signal differences in amplitude and phase. For consistency two consecutive measurements of A_{xy} are carried out through the method described above. To reduce the noise effect which might affect the amplitude level of the signals the IF bandwidth is set to 10 Hz. To reduce phase instability due to thermal drift between the signals measurements which is around 10° during the first 10-15 minutes and to avoid the VNA settling effect, another scan is conducted before the measurements of A_{xy} factors are performed. The first measurement of A_{xy} shows values of 1.48 dB for the amplitude and around -14° for phase, and 1.53 dB and around -8° , for the second measurement of A_{xy} . At 60 GHz these phase values correspond to a change in the path length between the two ports of the OMT, ranging between 0.11 mm and 0.19 mm. It can be noted that the amplitude and phase factors measurement results are not equal to 1, as it would be in the ideal case.

V. CONCLUSIONS

A dual-polarized probe at 60 GHz was implemented - a 27dBi conical horn - based on a SPDT switch up to 67 GHz and an OMT operating within (50-75) GHz frequency band, both components with isolation below -40 dB in the whole band. The conical horn was designed by conducting WIPL-D simulations and in-house manufactured. The probe system was assembled and tested as an AUT in the PNF setup at DTU. Probe pattern measurements were conducted without the switch in the first stage and then with the switch. For validation the results were compared with WIPL-D simulations indicating a good agreement, down to -30 dB pattern levels for $\phi = 0^\circ$, $\phi = 90^\circ$, $\phi = 45^\circ$ and $\phi = 135^\circ$ planes for the co-polar components and for the cross-polar down to -40 dB for $\phi = 45^\circ$ and $\phi = 135^\circ$ cuts. The cross-polar level indicates values below -32 dB on axis for the $\phi = 0^\circ$ and $\phi = 90^\circ$ planes. Radiation pattern of the probe tested with the switch was compared to the data without the switch showing a good agreement within the main beam region with some small differences below -30 dB levels due to the attenuation introduced by the switch. Channel balance was carried out in which two consecutive measurements of the amplitude phase factors were conducted showing 1.53 dB and 1.48 dB values in amplitude and between -14° and -8° values for phase. The phase difference in the results corresponds to a path length change between the OMT ports of 0.11 mm and 0.19 mm. According to the amplitude phase factors measurement results a correction factor will be applied on the measured data. The next step in the dual-polarized probe testing involves first-order performance investigation and testing of the probe in DTU ESA-SNF Facility: probe calibration and also using the probe as a probe to measure 60 GHz AUTs.

REFERENCES

- [1] L.J. Foged, A. Giacomini, R. Morbidini, V. Schirosi, S. Pivnenko, "Dual Polarized Near Field Probe Based on OMJ in Waveguide Technology Achieving More Than Octave Bandwidth", *36th Annual Symposium of the Antenna Measurement Technique Association*, October 12-17, Tucson, Arizona, 2014
- [2] Pieter N. Betjes, Danil J. Janse van Rensburg, Stuart F. Gregson, "An articulated Swing Arm System for Spherical Near Field Antenna Measurements at Millimeter Wave Frequencies", *ESA/ESTEC*, October 6-9, Noordwijk, The Netherlands, 2015
- [3] Joshua A. Gordon, Member, David R. Novotny, Michael H. Francis, Ronald C. Wittmann, Miranda L. Butler, Alexandra E. Curtin, Jeffery R. Guerrieri, "Millimeter-Wave Near-Field Measurements Using Coordinated Robotics", *IEEE Transactions on Antennas and Propagation*, vol. 63, no. 12, December 2015
- [4] J.E. Hansen, "Spherical Near-Field Antenna Measurements", *Peter Peregrinus Ltd*, London United Kingdom, 1988
- [5] S. Gregson, J. McCormick and C. Parini, "Principles of Planar Near-Field Antenna Measurements", *Institution of Engineering and Technology*, London 2007
- [6] P.I. Popa, S. Pivnenko, J.M. Nielsen, O. Breinbjerg, "60 GHz Antenna Measurement Setup using a VNA without External Frequency Conversion", *36th Annual Symposium of the Antenna Measurement Technique Association*, October 12-17, Tucson, Arizona, 2014
- [7] WIPL-D, <https://www.wipl-d.com/>
- [8] Millitech Inc., <http://www.millitech.com/>